

# Introduction

- **Transport modeling of toroidal plasmas**
  - To predict time evolution of burning plasmas
  - To develop reliable and efficient control schemes

- **Various Levels of Transport Analyses**

- Diffusive Transport Model
- Dynamical Transport Model
- Kinetic Transport Model

- **Most of present transport analyses**

- Diffusive transport model based on the flux-gradient relations
- The Maxwellian velocity distribution for bulk species
- Success in reproducing the formation of ITB

- **Dynamical transport model**

- To describe rapid transition in transport barrier formation
- Self-consistent analysis of plasma rotation and radial electric field
- Consistent analysis of neoclassical and turbulent transports

- **Kinetic Transport Model**

- Deviation from Maxwellian due to heating and current drive
- Velocity dependence of transport coefficients and instabilities
- Poloidal angle dependence of radial flux

## Integrated Modeling of Toroidal Plasmas

- **TASK code** (Transport Analysing System for Tokamak)
- **Modular structure, Standard data interface, Portable**

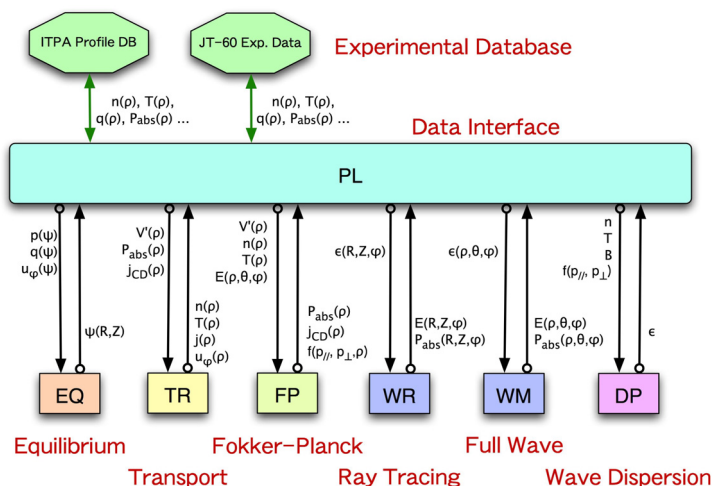


FIG. 1. Modular structure of TASK code system

# Diffusive Transport Analysis

- Based on the flux-gradient relations derived from stationary force balance:  $q = -\overline{\chi} \cdot \nabla T$

## Comparison of turbulent transport models

- Ballooning mode model: CDBM[1,2]
- ITG mode model: GLF23[3], IFS-PPPL[4], and Weiland model[5]

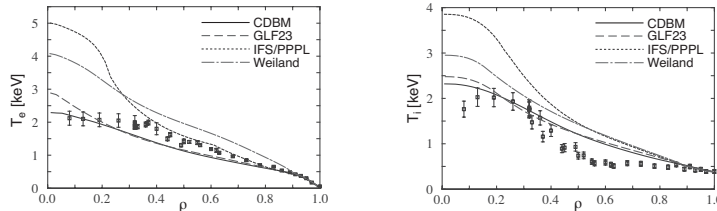


FIG. 2. Heat transport simulation for the L-mode shot #82188 on DIII-D tokamak.

## Steady state ITB simulation

- CDBM transport model including velocity shearing rate
- Radial electric field calculated from the radial force balance

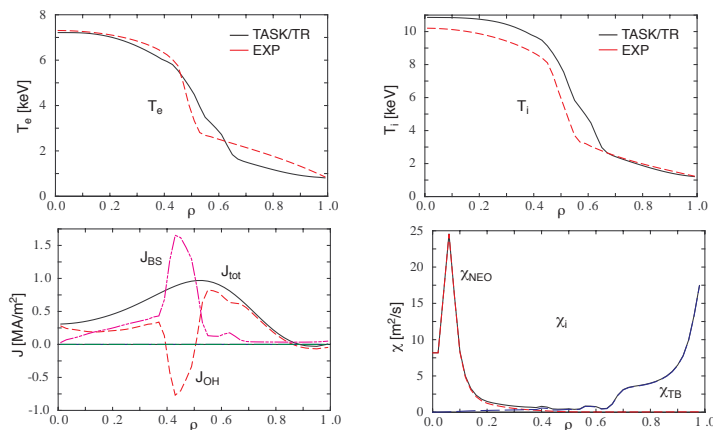


FIG. 3. Heat transport simulation for the ITB shot #29728 on the JT-60U Tokamak

## New transport model

- A set of model equations describing both the electrostatic toroidal ion temperature gradient mode and the electromagnetic ballooning mode was derived and turbulent transport coefficients was evaluated from the marginal stability condition of the most unstable mode [6].

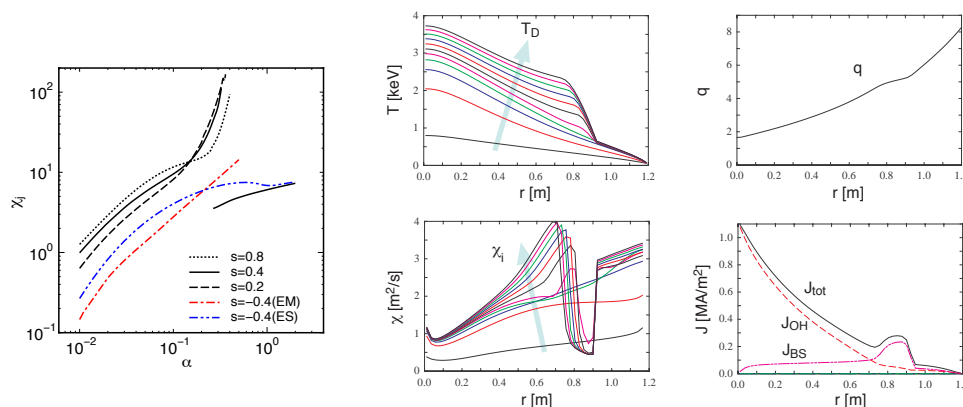


FIG. 4. Pressure gradient dependence of the transport coefficients for various values of  $s$  and Radial profiles in the high- $\beta_p$  operation mode.

# Dynamical Transport Analysis

## Basic equations [TASK/TX]

- **Toroidal coordinates**  $(r, \theta, \phi)$  and **toroidal plasma**
- **Surface-averaged two-fluid equations for the density**  $n_s$ , **radial flow**  $u_{sr}$ , **poloidal rotation**  $u_{s\theta}$  and **toroidal rotation**  $u_{s\phi}$  and **Maxwell's equations are solved.**

$$\frac{\partial n_s}{\partial t} = -\frac{1}{r} \frac{\partial}{\partial r} r n_s u_{sr} + S_s$$

$$\frac{\partial}{\partial t} m_s n_s u_{sr} = \frac{1}{r} m_s n_s u_{s\theta}^2 + e_s n_s (E_r + u_{s\theta} B_\phi - u_{s\phi} B_\theta) - \frac{\partial}{\partial r} n_s T_s$$

$$\frac{\partial}{\partial t} m_s n_s u_{s\theta} = e_s n_s (E_\theta - u_{sr} B_\phi) + \frac{1}{r^2} \frac{\partial}{\partial r} r^3 n_s m_s \mu_s \frac{\partial}{\partial r} \frac{u_{s\theta}}{r} + F_{s\theta}^{\text{NC}} + F_{s\theta}^{\text{C}} + F_{s\theta}^{\text{W}} + F_{s\theta}^{\text{X}} + F_{s\theta}^{\text{L}}$$

$$\frac{\partial}{\partial t} m_s n_s u_{s\phi} = e_s n_s (E_\phi + u_{sr} B_\theta) + \frac{1}{r} \frac{\partial}{\partial r} r n_s m_s \mu_s \frac{\partial}{\partial r} u_{s\phi} + F_{s\phi}^{\text{NC}} + F_{s\phi}^{\text{C}} + F_{s\phi}^{\text{W}} + F_{s\phi}^{\text{X}} + F_{s\phi}^{\text{L}}$$

$$\frac{\partial}{\partial t} \frac{3}{2} n_s T_s = -\frac{1}{r} \frac{\partial}{\partial r} r \left( \frac{5}{2} u_{sr} n_s T_s - n_s \chi_s \frac{\partial}{\partial r} T_e \right) + e_s n_s (E_\theta u_{s\theta} + E_\phi u_{s\phi}) + P_s^{\text{C}} + P_s^{\text{L}} + P_s^{\text{H}}$$

where  $m_s$  and  $e_s$  are the mass and charge of particle species  $s$ . The particle source and sink,  $S_s$ , neoclassical viscosity force,  $F^{\text{NC}}$ , collisional momentum transfer,  $F^{\text{C}}$ , force due to the interaction with turbulent electric field,  $F^{\text{W}}$ , charge exchange force on ions,  $F^{\text{X}}$ , and loss along the field line in the SOL region ( $r/a > 1$ ),  $F^{\text{L}}$ , are calculated from local quantities[8]. The perpendicular viscosity,  $\mu_s$ , and thermal conductivity,  $\chi_s$ , represent anomalous transport due to the turbulence. Neoclassical effect is included as a poloidal viscosity in tokamaks and both poloidal and toroidal viscosities in helical systems.

## Neoclassical transport at the edge generates $E_r$ and barrier

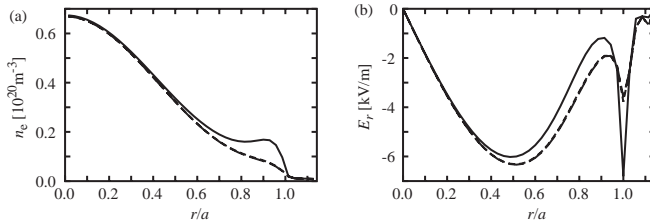


FIG. 5. Radial profiles of the density and  $E_r$  with (dashed lines) and without (solid lines) turbulent transport.

## Edge transport barrier is sensitive to the edge temperature

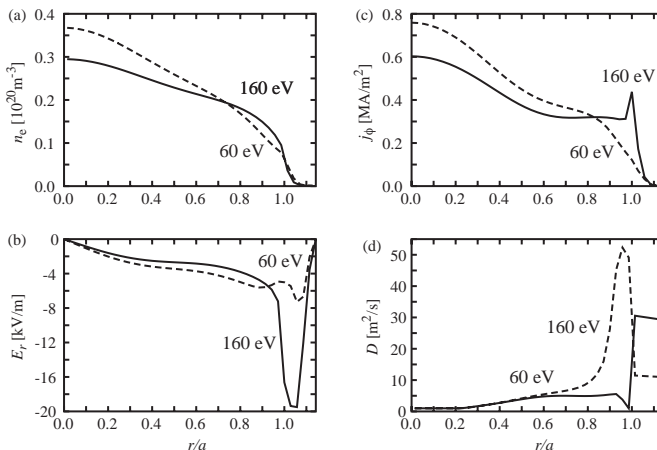


FIG. 6. Edge temperature dependence of radial profile

## Effect of neoclassical toroidal viscosity in a helical device

- The toroidal rotation speed is one order of magnitude lower than that of tokamaks.

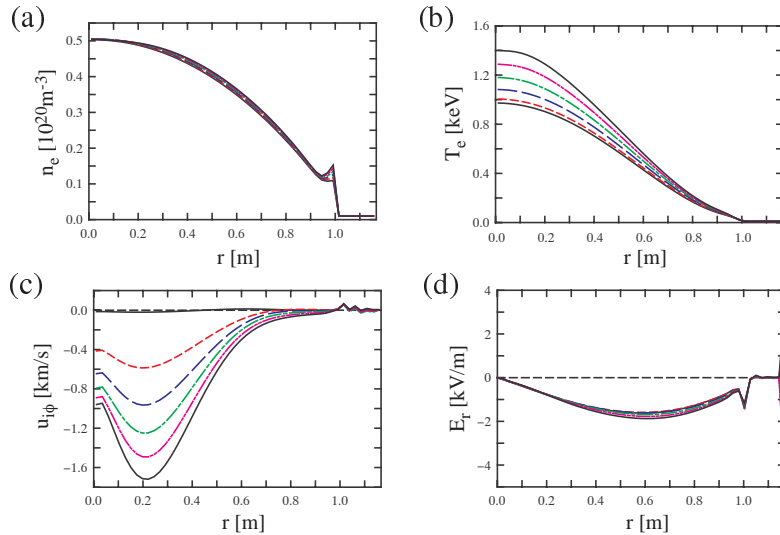


FIG. 7. Transport simulation of a helical plasma with NB injection

## Kinetic Transport Analysis

The velocity distributions in a fusion plasma will not be necessarily close to the Maxwellian and affect the transport, the heating power requirement for startup, and poloidal distribution of radial flux. The TASK code includes a three-dimensional bounce-averaged Fokker-Planck module TASK/FP which has been used for the analysis of electron cyclotron heating and current drive. This module has been extended to describe the time evolution of non-Maxwellian velocity distribution in a transport time scale. We have formulated the neoclassical radial diffusion and parallel force driven by the spatial gradient. Turbulent diffusion in velocity space and radius will be also implemented. The kinetic transport analysis may be a long-range task, but the framework of the integrated modeling code should be prepared for such advanced analyses.

**Acknowledgements** This work is supported by Grant-in-Aid for Scientific Research from JSPS and Grant-in-Aid for Specially Promoted Research from MEXT. It is also a part of the collaboration research program between universities and JAERI and the joint research program of RIAM, Kyushu University. AF and MH would like to thank Dr. T. Takizuka and Dr. Y. Sakamoto of JAERI for valuable discussions and Dr. J. Weiland for his help in implementing his modes. We also appreciate the international tokamak profile database and the NTCC code library.

### References

- [1] FUKUYAMA, A., et al.: Plasma Phys. Control. Fusion **37** (1995) 611-631.
- [2] ITOH, K., et al.: Plasma Phys. Control. Fusion **36** (1994) 279-306.
- [3] WALTZ, R. E., et al.: Phys. Plasmas **4** (1997) 2482.
- [4] KOTSCHENREUTHER, M., et al.: Phys. Plasmas **2** (1995) 2381.
- [5] WEILAND, J., JARMAN, A., NORDMAN, H.: Nucl. Fusion **29** (1989) 1810.
- [6] UCHIDA, M., FUKUYAMA, A., Proc. of 30th EPS Conf. on Control. Fusion and Plasma Phys. (St. Petersburg, 2003) P-2.118.
- [7] FUKUYAMA, A., UCHIDA, M., HONDA, M., 9th IAEA TM on H-mode Physics and Transport Barriers (San Diego, 2003) C1.
- [8] FUKUYAMA, A., FUJI, Y., ITOH, K., ITOH, S.-I., Plasma Phys. Control. Fusion **36** (1994) A159-A164.
- [9] FUKUYAMA, A., FUJI, Y., ITOH, S.-I., YAGI, M., ITOH, K., Plasma Phys. Control. Fusion **38** (1996) 1319-1322.
- [10] ITOH, S.-I., ITOH, K., FUKUYAMA, A., YAGI, M., Phys. Rev. Lett. **72** (1994) 1200-3.